Article

Discovery Medicine 2024; 36(181): 278–285
https://doi.org/10.24976/Discov.Med.202436181.26

The Value of Computed Tomography in Differentiating Heterotopic Pancreas from Small Gastrointestinal Stromal Tumor

Xiaolin Cui[1], Xinying Cong[2], Xuejing Liu[1,*]

[1]Department of Radiology, Beijing Friendship Hospital, Capital Medical University, 100050 Beijing, China
[2]Department of Radiology, China Rehabilitation Research Center, 100068 Beijing, China
*Correspondence: jxliu1029@126.com (Xuejing Liu)
Published: 20 February 2024

Background: It is critical for an accurate preoperative diagnosis of heterotopic pancreas (HP) and small gastrointestinal stromal tumor (GIST), given the unique treatment and prognosis of the two tumors. This study aims to investigate HP's computed tomography (CT) features and identify the distinguishing characteristics between HP and small GIST.
Methods: From January 2016 to August 2020, our hospital database was searched for confirmed histopathological results and CT scans for HP and GIST for further analysis. The statistically significant variables were determined by using Fisher's exact test, the Mann-Whitney U test, the receiver operating characteristic (ROC) curve and the inverse probability weighting method.
Results: CT images and clinical data were reviewed for 24 participants with HP and 34 patients with small GIST. Contour, border, relative enhancement grade, surface dimple, duct-like structure, short diameter (SD), attenuation of each lesion in the unenhanced phase (Lp), and the enhancement ratio of tumor in the venous phase (ER) were significant for differentiating HP from small GIST. Threshold values for SD and Lp were 1.40 cm and 42.33 Hounsfield units, respectively. Ill-defined border, surface dimple, ductlike structure, and Lp were independent factors that differentiated HP from small GIST. Additionally, SD and ER were also found to be independent factors.
Conclusions: Contour, relative enhancement grade, SD, and Lp could effectively differentiate HP from small GIST, demonstrating improved diagnostic performance compared to other parameters. The presence of ductlike structures and surface dimples could further characterize HP. These findings may help distinguish HP from small GIST and avoid unnecessary invasive examination and therapy in individuals with asymptomatic HP.

Keywords: heterotopic pancreas; computed tomography; gastrointestinal stromal tumor; diagnosis

Introduction

Heterotopic pancreas (HP), commonly located in the stomach, duodenum, and proximal jejunum, is defined as isolated pancreatic tissue outside the normal pancreas and without any vascular and anatomic continuity [1–4]. This tumor is usually discovered incidentally during an unrelated operation or imaging evaluation, as most of the lesions are generally asymptomatic. However, in some cases, a few lesions are detected because of clinical symptoms caused by complications such as pancreatitis, pseudocyst, and tumor [5,6].

HP is usually found in the submucosa of the gastrointestinal tract. HP smaller than 4 cm in diameter can be easily misdiagnosed as gastrointestinal stromal tumor (GIST), the most common submucosal tumor [3,7,8]. The treatment and prognosis between HP and GIST are quite different. HP is described as a nearly benign lesion that requires follow-up. GIST, however, is thought to have malignant potential, as this tumor can recur locally and spread to the liver and peritoneum. Accordingly, surgery is the first choice of treatment for GIST, and administration of tyrosine kinase inhibitors is required if metastasis occurs [9,10]. Hence, an accurate preoperative diagnosis is necessary for HP and GIST. Since HP and GIST share similar clinical presentations, only relying on clinical symptoms for diagnosis is problematic. Previous studies have shown that computed tomography (CT), the most routinely used noninvasive imaging examination, is essential in the preoperative evaluation of gastrointestinal tumors [11,12]. Currently, a few studies have reported CT findings of patients with HP and identified characteristics that distinguish HP from GIST, such as location, contour, and margin [3,7,8]. However, these investigations mostly focused on CT-based morphologic HP analysis, and the conclusions need further confirmation. Additionally, previous studies did not employ logistic regression analysis, which could reveal more reliable diagnostic characteristics between HP and GIST [3,7,8]. Therefore, in this retrospective study, the authors aimed to describe CT findings of HP and to determine in-

dependent factors that differentiate HP from GIST by using the inverse probability (IP) weighting method.

Materials and Methods

Patients

This retrospective study was approved by the Review Committee of Beijing Friendship Hospital, Capital Medical University (2023-P2-308-01). And informed consent for CT scanning was obtained from each participant included in this study. The hospital database was searched to identify pathological results for HP and GIST between January 2016 and August 2020. Initially, a total of 498 patients were found, including 63 patients with HP and 435 with GISTs. Inclusion criteria for our study were as follows: (1) surgical resection of lesions and a histopathologic diagnosis of HP or GIST; (2) availability of patients' contrast-enhanced and reconstructed CT images; (3) presence of a single lesion; and (4) lesions less than 4 cm in diameter to avoid potential bias caused by size differences, as most previously reported cases of HP, including those presenting at our hospital had tumors smaller than 4 cm. Among the 498 patients, 359 patients with GIST larger than 4 cm in diameter were excluded at imaging measurement. Additionally, 39 HP tumors and 42 GISTs were excluded due to a lack of CT images. Consequently, 24 patients with HP (14 men and 10 women) and 34 with GIST (19 men and 15 women) were included in this study (Fig. 1).

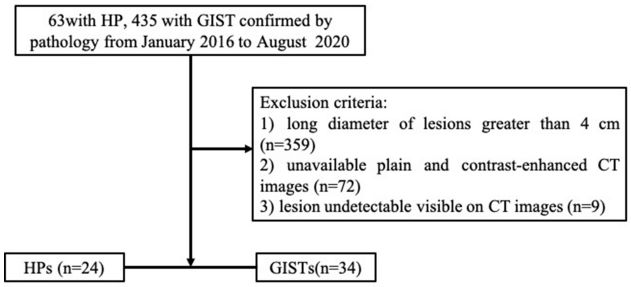

Fig. 1. Flowchart of patients included in the study. HP, heterotopic pancreas; GIST, gastrointestinal stromal tumor; CT, computed tomography.

CT Technique

All CT examinations were performed using a GE Discovery CT750 HD scanner (GE Healthcare, Waukesha, WI, USA). CT images were obtained with the following parameters, as patients held their breath: 120 kVp; automatic mA; pitch coefficient, 0.984; collimator width, 40 mm; slice thickness, 5 mm; and display field-of-view, 25–30 cm. Scanning ranged from the dome of the diaphragm to the level of the kidneys. For the contrast-enhanced CT scan, 450 mg I/kg of iodine (Omnipaque-350, GE Healthcare, Chicago, IL, USA) was injected intravenously at a flow rate of 3 mL/s via a power injector. The arterial phase acquisition was performed using the bolus-tracking technique. The region of interest (ROI) was placed in the descending thoracic aorta. When the CT value of the ROI reached 100 Hounsfield units (HU), a scan was automatically triggered after a delay of 7 s. The portal venous phase was obtained 30 s after the end of the arterial phase. All patients underwent dual-phasic CT, which included unenhanced, arterial, and portal phase scanning. All images were reconstructed in the axial plane at a slice thickness of 1.25 mm and an interval of 1.25 mm.

Imaging Analysis

All CT images were assessed after consensus by two experienced radiologists with 8 and 6 years of expertise in abdominal CT diagnosis, who were blinded to the surgical and histopathologic results. They reviewed CT images at Advantage workstation (version 4.6, GE Healthcare, Milwaukee, WI, USA).

Qualitative Analysis

For all lesions, the following CT morphologic parameters were evaluated: (1) location; (2) contour; (3) growth pattern; (4) lesion border; (5) enhancement pattern and degree; (6) the presence of surface dimples; (7) prominent enhancement of the overlying mucosa; and (8) the presence of a ductlike structure [13]. Lesions were recorded as bell-shaped, round, ovoid, dumbbell, or flat [3,8]. Growth patterns were classified as endoluminal, exoluminal, or mixed [3,8]. Enhancement patterns (homogeneous versus heterogeneous) were evaluated, and the relative enhancement degree (high, intermediate, or low) of the lesions was compared to the enhancement of the main pancreas in the arterial phase. In addition, tumor-related complications were also analyzed.

Quantitative Analysis

The long diameter (LD) and the short diameter (SD) of all lesions were measured, and the aspect ratios (LD/SD) were calculated. To evaluate the relative degree of enhancement in the two types of tumors, CT attenuation values (HU) of lesions (L), as well as the abdominal aortas (A) in the same layer and the pancreas (P), were measured in the unenhanced phase (p), arterial phase (a), and venous phase (v) using 10–20 mm^2 circular ROIs. The ROI was carefully drawn in the solid portion of the lesion, avoiding adjacent structures. An average of three measurements per lesion (abdominal aorta and pancreas) were performed. CT attenuation values of the tumors (abdominal aortas and pancreas) were recorded as Lp (Ap and Pp), La (Aa and Pa), and Lv (Av and Pv), respectively. To standardize CT values of the lesions with different injection rates and doses, as well as individual circulation levels in different patients, the Lp/Ap (Sp), La/Aa (Sa), and Lv/Av (Sv) ratios were further calculated [8]. Moreover, the tumor enhance-

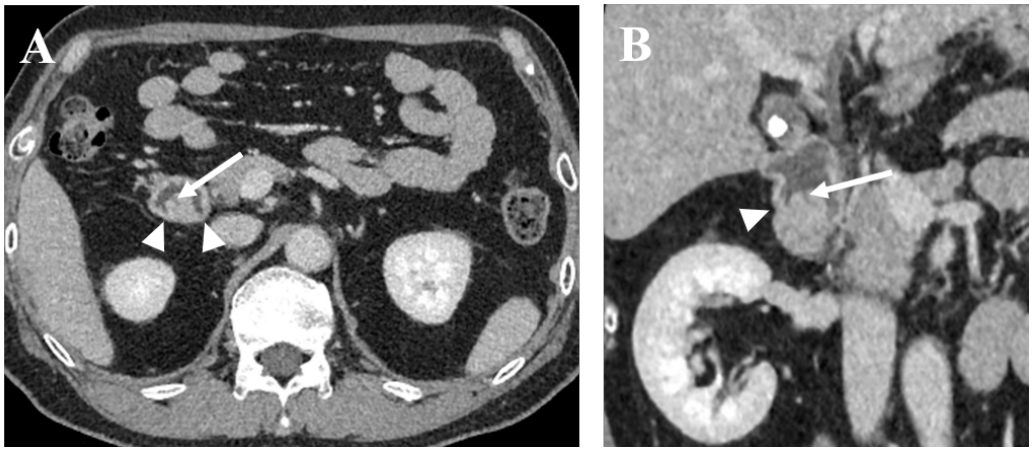

Fig. 2. Heterotopic pancreas in the duodenum in a 60-year-old woman. Axial (A) and coronal (B) portal venous phase CT images showed a 1.3 cm, ill-defined, bell-shaped (arrowheads), endoluminal intramural mass with homogeneous enhancement in the duodenum (similar to the enhancement of the orthotopic pancreas). A small ductlike structure (white arrows) was observed within the lesion, extending to the surface.

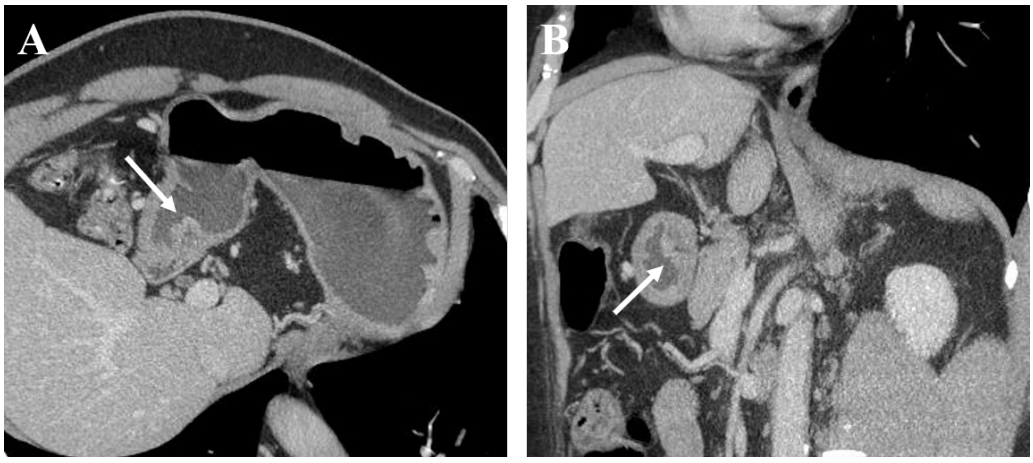

Fig. 3. Heterotopic pancreas (HP) in the stomach antrum in a 51-year-old man. Oblique coronal (A), and sagittal (B) contrast-enhanced CT images acquired in the portal venous phase showed a solid intramural mass with heterogeneous enhancement in the stomach antrum (similar to the enhancement of the orthotopic pancreas). Note surface dimple (white arrows).

ment value ($HU_{arterial} - HU_{plain}$, $HU_{venous} - HU_{plain}$), the tumor enhancement ratio (ERa [$HU_{arterial} - HU_{plain}/HU_{plain}$], ER [$HU_{venous} - HU_{plain}/HU_{plain}$]), and the tumor enhancement ratio to pancreas in the arterial and venous phases ($HU_{tumor}/HU_{pancreas}$, ERPa, and ERPv) were also calculated [7].

Statistical Analysis

To assess categoric variables between HP and small GIST including demographic data (sex and presentation) and qualitative CT features, Fisher's exact tests were used. Due to the non-normal distribution of patients' age and quantitative CT characteristics as determined by the Shapiro-Wilk test, the Mann-Whitney U test was employed to analyze these continuous variables. The diagnostic performance was analyzed using receiver operating characteristic (ROC) analysis, and we chose an appropriate threshold value which yielded a threshold level with high sensitivity and specificity. Independent factors focused on differentiating between patients with HP and small GIST were identified using the IP weighting method. Data on patients' demographics, presenting symptoms, and CT results were abstracted directly from patient medical records. Using CT results as exposure factors of interest, we applied the IP weighting method to determine these independent factors. In detail, the IP weighting method removes confounding information by creating a pseudo-population, in which the probability of interest exposure is predicted via a logistic regression on the basis of diagnosis age, sex, symptoms, contour, growth pattern, border, enhancement pattern, enhancement grade, prominent enhancement of overlying mucosa, surface dimple, and duct-like structure, referred as P[E|L]. Thus, the IP weighting for patients being assigned

Table 1. Demographics, presentation, and follow-up data of 24 patients with HP and 34 patients with small GIST.

	HP (n = 24)	GIST (n = 34)	*p* value
Patient age (years), mean (range)	52.63 ± 9.04	58.15 ± 9.33	0.015*
Sex distribution			0.787
Female	10 (41.67%)	15 (44.12%)	
Male	14 (58.33%)	19 (55.88%)	
Presentation			0.078
Abdominal pain or discomfort	10 (41.67%)	15 (44.12%)	
Asymptomatic	13 (54.17%)	11 (32.35%)	
Digestive tract hemorrhage	1 (4.16%)	8 (23.53%)	
Follow-up period (m), mean (range)	20.63 (2–55)	20.44 (3–40)	0.67

GIST, gastrointestinal stromal tumor; HP, heterotopic pancreas; m, month.

*$p < 0.05$.

to the exposed group was 1/Pr[E|L], and that for the unexposed group was 1/(1-Pr[E|L]). In practice, to improve the accuracy (i.e., the narrower range of the IP weights) of the estimates, stabilized weights are recommended, in which the re-estimated weight for patients in the exposed group was Pr(E=1)/Pr(E=1|L) and that for patients in the unexposed group was (1-Pr(E=1))/(1-Pr(E=1|L)).

For statistical analysis, we used SPSS Statistics (version 26.0; IBM Corp, Chicago, IL, USA), MedCalc (Version 19.0.6; MedCalc Software bv, Ostend, Belgium), and R (version 3.6.3, R Foundation for Statistical Computing, Vienna, Austria).

Results

Clinical Information

Table 1 shows the clinical characteristics of all cases as well as follow-up data. Sex distribution or symptoms did not significantly differ between patients with HP and those with small GIST; however, age distribution was significantly different between the two groups (HP [mean age, 52.63 ± 9.04 years; range, 31–69 years] and small GIST [mean age, 58.15 ± 9.33 years; range, 37–73 years]; $p < 0.05$).

Morphologic Analysis

Table 2 summarizes the morphologic qualitative CT findings of HP and small GIST. Tumor location was not significantly different between patients with HP and small GIST. The relative enhancement grade was significantly different between these two groups ($p = 0.003$). Compared to the main pancreas, HP showed lower attenuation in the arterial phase (75.00%), while small GIST showed lower or higher attenuation (97.06%). The presence of surface dimples and ductlike structures were significant factors in differentiating HP from small GIST (29.17% versus 0%, $p = 0.001$). In addition, one case with HP was complicated by pseudocyst formation which was preoperatively misdiagnosed as a cystic-solid mass of the pancreas. No other cases were complicated with acute pancreatitis or benign and malignant neoplasms. No evidence of recurrence or metastasis was observed in any patient. Representative images are presented in Figs. 2,3.

The SD and LD of HP masses were both smaller than those of small GIST (SD [HP = 1.34 ± 0.45 cm, small GIST = 1.87 ± 0.57 cm]; LD [HP = 1.95 ± 0.75 cm, small GIST = 2.35 ± 0.68 cm]), with SD being significantly different between the groups ($p < 0.05$). The LD/SD ratio for HP masses was higher than that of small GIST (HP = 1.45 ± 0.32, GIST = 1.28 ± 0.22), but the values were not significantly different. In the unenhanced phase, HP showed higher mean CT attenuation than small GIST (45.42 ± 9.05 HU for HP versus 37.41 ± 4.51 HU for GIST; $p < 0.05$), and Sp exhibited the same trends. HP had significantly higher ER than small GIST (1.59 ± 0.92 versus 1.12 ± 0.44). La, Lv, Sa, Sv, enhancement value, ERa, ERPa, and ERPv showed no significant differences between groups.

Sensitivity and Specificity Values for CT Diagnosis

Tables 3,4 summarize the sensitivity and specificity of each important CT finding in differentiating HP from small GIST. SD, Lp, and Sp had areas under ROC curves (AUC) greater than 0.7, and demonstrated better performance than other parameters in the differential diagnosis of HP from small GIST (Fig. 4). Additionally, Lp and Sp had AUCs of 0.813 and 0.813, respectively, indicating the greatest ability of this differentiation. The threshold values for SD, Lp, Sp, and ER were 1.40 cm, 42.33 HU, 0.93, and 0.97, respectively. When five CT findings, including contour, enhancement grade, SD, Lp, and Sp were used in combination, the sensitivity and specificity for differentiating HP from small GIST were 83.3% and 91.2%, respectively.

The IP weighting method was used to identify independent factors that distinguish individuals with HP from those with small GIST (Table 5). Further, we found that border, presence of surface dimples and ductlike structures, SD, Lp, Sp, and ER were independent factors. Furthermore, ill-defined border, the presence of surface dimples and ductlike structures, Lp, and Sp were all suggestive imaging findings of HP.

Table 2. Morphologic qualitative CT findings of heterotopic pancreas and small gastrointestinal stromal tumor.

CT finding	HPs (n = 24)	GISTs (n = 34)	*p* value
Location			0.33
Cardia	0 (0.00%)	0 (0.00%)	
Fundus	0 (0.00%)	5 (14.71%)	
Body	7 (29.17%)	11 (32.35%)	
Angle	0 (0.00%)	0 (0.00%)	
Antrum	5 (20.83%)	6 (17.65%)	
Duodenum	10 (41.67%)	11 (32.35%)	
Jejunum/ileum	2 (8.33%)	1 (2.94%)	
Contour			0.001*
Bell-shaped	7 (29.17%)	7 (20.59%)	
Round	5 (20.83%)	11 (32.35%)	
Ovoid	4 (16.67%)	9 (26.47%)	
Dumbbell	0 (0.00%)	7 (20.59%)	
Flat	8 (33.33%)	0 (0.00%)	
Growth pattern			0.151
Endoluminal	16 (66.67%)	14 (41.18%)	
Exophytic	3 (12.50%)	8 (23.53%)	
Mixed	5 (20.83%)	12 (35.29%)	
Border			0.001*
Ill-defined	15 (62.50%)	6 (17.65%)	
Well-defined	9 (37.50%)	28 (82.35%)	
Enhancement pattern			0.333
Heterogeneous	3 (12.50%)	8 (23.53%)	
Homogeneous	21 (87.50%)	26 (76.47%)	
Enhancement grade			0.003*
Similar to normal pancreas	5 (20.83%)	1 (2.94%)	
Lower to normal pancreas	18 (75.00%)	21 (61.77%)	
Higher to normal pancreas	1 (4.17%)	12 (35.29%)	
Surface dimple	7 (29.17%)	0 (0.00%)	0.001*
Prominent enhancement of overlying mucosa	7 (29.17%)	9 (26.47%)	1.00
Duct-like structure	7 (29.17%)	0 (0.00%)	0.001*

CT, computed tomography; GIST, gastrointestinal stromal tumor; HP, heterotopic pancreas.
*$p < 0.05$.

Discussion

In this study, nine CT features, including contour, border, relative enhancement grade, surface dimples, ductlike structures, SD, Lp, Sp, and ER were considered significant predictors for distinguishing HP from small GIST. Furthermore, the combination of these CT imaging findings can improve the accuracy of differential diagnosis between the two tumors. Additionally, ill-defined border, presence of surface dimples and ductlike structures, Lp, and Sp were identified as independent factors using the IP weighting method. The findings of this study may help distinguish HP from small GIST, potentially allowing patients with asymptomatic HP to avoid unnecessary and invasive examination and therapy.

In this study, 62.5% (15/24) of HP scans appeared bell-shaped or as flat masses, whereas 58.8% GISTs were more likely to be round or ovoid (20/34). Our results also showed that the SD of HP masses was significantly smaller than that of small GIST. This finding may be related to the pathological tissue of HP, which is ectopic flat glandular tissue with pancreatic acinar formation and duct development [13–16]. Further, this result may also explain why HP has an ill-defined margin. Of the 24, 15 (62.5%) HPs showed an ill-defined border at CT imaging in our investigation, which is similar to those reported with previous studies [2,3,7,8]. Unlike previous research, the tumor site was not found to be a distinguishing feature between HP and small GIST in the present study [2,3,7,8]. This inconsistency in results might largely be due to differences in patient enrollment patterns and the degree of distention of the upper gastrointestinal tract [8,17].

In our study, the ductlike structure was only found in patients with HP (7 of 24, 29.2%). Moreover, the IP weighting method indicated that ductlike structure was an independent factor that differentiated HP from small GIST. Therefore, this feature is probably a vital finding for the diagnosis of HP. Previous research indicates this feature corresponds

Table 3. The diagnostic performance of CT findings in distinguishing heterotopic pancreas from small gastrointestinal stromal tumors.

CT finding	Sensitivity (%)	Specificity (%)	Cutoff value
Contour (dumbbell)	0	50	—
Contour (flat)	33.3	100	—
Border	66.7	58.8	—
Enhancement grade	20.8	97.1	—
Surface dimple	29.2	100	—
Duct-like structure	29.2	100	—
SD	58.3	70.6	1.4
Lp	70.8	79.4	42.33
Sp	70.8	73.5	0.93
ER	50	76.5	0.97

CT, computed tomography; SD, short diameter; Lp, CT attenuation value of each lesion in the unenhanced phase; Sp, attenuation of lesion/attenuation of abdominal aortas in the unenhanced phase; ER, enhancement ratio in the venous phase.

Table 4. The diagnostic performance of combined CT findings in distinguishing heterotopic pancreas from gastrointestinal stromal tumors.

Combined CT finding	Sensitivity (%)	Specificity (%)
Lp+Sp+SD	66.7	82.4
Contour+enhancement grade	45.8	97.1
Lp+Sp+SD+contour+enhancement grade	83.3	91.2

CT, computed tomography.

to a dilated duct in HP, also known as the "ectopic duct" sign [5,8]. The "ectopic duct" sign was frequently observed in enhanced CT three-dimensional reconstruction in individuals with HP, as described in Cai's study [8]. Enhanced three-dimensional CT reconstruction, which is superior to unenhanced axial imaging, clearly shows ductal structure from multiple angles to avoid the volume effect, improving the degree of diagnostic accuracy of HP.

Several radiologic-pathologic studies indicated that the grade and pattern of HP enhancement correlate with its histologic composition [4,5,18–21]. Acini-dominated lesions are more homogeneous and show greater enhancement than other lesion types. In this study, both HP and GIST showed predominantly homogeneous enhancement. The relative enhancement grade between HP and GIST was significant, as reported in previous studies [7,8]. However, Kim *et al.* [3] found no statistical difference in the relative enhancement grade between these two tumors. In addition, this study used semiquantitative parameters to analyze the differences in unenhanced CT values and enhanced CT values among heterotopic pancreas and GIST. Lp >42.33 HU, Sp >0.93, and ER >0.97 were significant semiquantitative CT features for distinguishing HP from GIST ($p < 0.05$), which was consistent with previous CT imaging findings

Table 5. Independent effect of exposure of interest on pathological type using the inverse probability weighting method.

Exposure	OR (95% CI)	*p* value	Index
Border	1.49 (1.12–1.99)	0.006	Ill defined
Surface dimple	0.51 (0.43–0.61)	0.000	Not exist
Duct-like structure	0.51 (0.43–0.61)	0.000	Not exist
SD	0.68 (0.56–0.83)	0.000	SD
Lp	1.04 (1.02–1.06)	0.000	Lp
Sp	4.42 (2.02–9.67)	0.000	Sp
ER	0.81 (0.69–0.95)	0.012	ER

CI, confidence interval; ER, enhancement ratio in the venous phase; Lp, CT attenuation value of each lesion in the unenhanced phase; OR, odds ratio; Sp, ratio of CT attenuation values of lesions and values of abdominal aortas in the unenhanced phase.

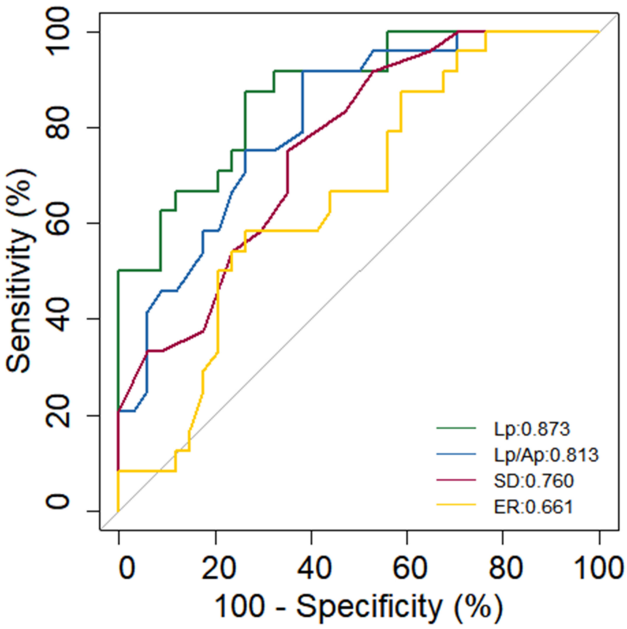

Fig. 4. Receiver operating characteristic (ROC) curves of Lp, Lp/Ap, SD, and ER in distinguishing heterotopic pancreas (HP) from small gastrointestinal stromal tumor (GIST). Lp, Lp/Ap, and SD are shown to have better diagnostic performance than other parameters for differentiating HP from small GIST.

[7,8]. Lp and Sp had a higher sensitivity than ER, indicating CT of an HP mass in the unenhanced phase is more valuable for differentiating HP from GIST.

Of note, age distribution was significantly different between the two groups (HP [mean age, 52.63 ± 9.04 years; range, 31–69 years] and GIST [mean age, 58.15 ± 9.33 years; range, 37–73 years]; $p < 0.05$) in this study, aligning with previous research by Kim *et al.* [3]. This suggests that age plays a role in the differentiation between the two tumors.

This study has several limitations. Firstly, because this was a retrospective single-center analysis, selection and

hospitalization bias could not be avoided. Secondly, due to the low prevalence of HP, our study included a small sample size of individuals with HP. Thirdly, the radiologic-pathologic correlation was not fully assessed in our study because a complete pathological specimen was not available. Despite this, several radiologic-pathologic studies have indicated a correlation between CT scans and histological results, as mentioned above [3,7,8]. In addition, all CT images were assessed by two experienced radiologists in our study, which is subjective to some degree. As cases accumulate, the hope is that artificial intelligence technology can be utilized for more objective evaluation in the future.

Conclusions

Contour, relative enhancement grade, Lp, Sp, and SD may help to accurately distinguish HP from small GIST. Using the IP weighting method, ill-defined border, the presence of surface dimples and ductlike structures, Lp, and Sp were identified as independent factors. Additionally, the ductlike structures and surface dimples were observed only in individuals with HP. These two findings may be reliable markers for diagnosing HP. Three-dimensional CT reconstruction may be useful in distinguishing features of HP and small GIST to avoid unnecessary invasive examination and therapy in patients with asymptomatic HP.

Availability of Data and Materials

The datasets used or analyzed during the current study are available from the corresponding author on reasonable request.

Author Contributions

XLC, XJL: conception and design of the research; writing of the manuscript; critical revision of the manuscript for intellectual content. XYC: acquisition of data; statistical analysis. All authors contributed to editorial changes in the manuscript. All authors have read and approved the final manuscript and agreed to be accountable for all aspects of the work.

Ethics Approval and Consent to Participate

Written consent for computed tomography exams had routinely been obtained from each individual included in this study. This study followed the Declaration of Helsinki and was approved by the Review Committee of Beijing Friendship Hospital, Capital Medical University (2023-P2-308-01).

Acknowledgment

Not applicable.

Funding

This research received no external funding.

Conflict of Interest

The authors declare no conflict of interest.

References

[1] Borghei P, Sokhandon F, Shirkhoda A, Morgan DE. Anomalies, anatomic variants, and sources of diagnostic pitfalls in pancreatic imaging. Radiology. 2013; 266: 28–36.

[2] Rezvani M, Menias C, Sandrasegaran K, Olpin JD, Elsayes KM, Shaaban AM. Heterotopic Pancreas: Histopathologic Features, Imaging Findings, and Complications. Radiographics. 2017; 37: 484–499.

[3] Kim JY, Lee JM, Kim KW, Park HS, Choi JY, Kim SH, *et al*. Ectopic pancreas: CT findings with emphasis on differentiation from small gastrointestinal stromal tumor and leiomyoma. Radiology. 2009; 252: 92–100.

[4] Kim DW, Kim JH, Park SH, Lee JS, Hong SM, Kim M, *et al*. Heterotopic pancreas of the jejunum: associations between CT and pathology features. Abdominal Imaging. 2015; 40: 38–45.

[5] Kung JW, Brown A, Kruskal JB, Goldsmith JD, Pedrosa I. Heterotopic pancreas: typical and atypical imaging findings. Clinical Radiology. 2010; 65: 403–407.

[6] Fukino N, Oida T, Mimatsu K, Kuboi Y, Kida K. Adenocarcinoma arising from heterotopic pancreas at the third portion of the duodenum. World Journal of Gastroenterology. 2015; 21: 4082–4088.

[7] Li LM, Feng LY, Chen XH, Liang P, Li J, Gao JB. Gastric heterotopic pancreas and stromal tumors smaller than 3 cm in diameter: clinical and computed tomography findings. Cancer Imaging. 2018; 18: 26.

[8] Yang CW, Liu XJ, Wei Y, Wan S, Ye Z, Yao S, *et al*. Use of computed tomography for distinguishing heterotopic pancreas from gastrointestinal stromal tumor and leiomyoma. Abdominal Radiology. 2021; 46: 168–178.

[9] Casali PG, Abecassis N, Aro HT, Bauer S, Biagini R, Bielack S, *et al*. Gastrointestinal stromal tumours: ESMO-EURACAN Clinical Practice Guidelines for diagnosis, treatment and follow-up. Annals of Oncology. 2018; 29: iv267.

[10] von Mehren M, Kane JM, Bui MM, Choy E, Connelly M, Dry S, *et al*. NCCN Guidelines Insights: Soft Tissue Sarcoma, Version 1.2021. Journal of the National Comprehensive Cancer Network. 2020; 18: 1604–1612.

[11] Song Y, Li J, Wang H, Liu B, Yuan C, Liu H, *et al*. Radiomics Nomogram Based on Contrast-enhanced CT to Predict the Malignant Potential of Gastrointestinal Stromal Tumor: A Two-center Study. Academic Radiology. 2022; 29: 806–816.

[12] Mazzei MA, Cioffi Squitieri N, Vindigni C, Guerrini S, Gentili F, Sadotti G, *et al*. Gastrointestinal stromal tumors (GIST): a proposal of a "CT-based predictive model of Miettinen index" in predicting the risk of malignancy. Abdominal Radiology. 2020; 45: 2989–2996.

[13] Kilman WJ, Berk RN. The spectrum of radiographic features of aberrant pancreatic rests involving the stomach. Radiology. 1977; 123: 291–296.

[14] ROONEY DR. Aberrant pancreatic tissue in the stomach. Radiology. 1959; 73: 241–244.

[15] Milosavljevic T, Perisic V, Opric D, Micev M, Korneti V, Kovacevic N, *et al*. Ectopic pancreas in the gastric wall Ektopicni pankreas u zidu zeludca. Archives of Gastroenterohepatology. 2000; 19: 24–27.

[16] Matsumoto T, Tanaka N, Nagai M, Koike D, Sakuraoka Y, Kubota K. A case of gastric heterotopic pancreatitis resected by laparoscopic surgery. International Surgery. 2015; 100: 678–682.

[17] Jang KM, Kim SH, Park HJ, Lim S, Kang TW, Lee SJ, *et al*. Ectopic pancreas in upper gastrointestinal tract: MRI findings with emphasis on differentiation from submucosal tumor. Acta Radiologica. 2013; 54: 1107–1116.

[18] Lin YM, Chiu NC, Li AFY, Liu CA, Chou YH, Chiou YY. Unusual gastric tumors and tumor-like lesions: Radiological with pathological correlation and literature review. World Journal of Gastroenterology. 2017; 23: 2493–2504.

[19] Park SH, Han JK, Choi BI, Kim M, Kim YI, Yeon KM, *et al*. Heterotopic pancreas of the stomach: CT findings correlated with pathologic findings in six patients. Abdominal Imaging. 2000; 25: 119–123.

[20] Lee NK, Kim S, Kim GH, Jeon TY, Kim DH, Jang HJ, *et al*. Hypervascular subepithelial gastrointestinal masses: CT-pathologic correlation. Radiographics. 2010; 30: 1915–1934.

[21] Lee NK, Kim S, Jeon TY, Kim HS, Kim DH, Seo HI, *et al*. Complications of congenital and developmental abnormalities of the gastrointestinal tract in adolescents and adults: evaluation with multimodality imaging. Radiographics. 2010; 30: 1489–1507.